ORIGINAL ARTICLE

Biologically-based modeling of radiation risk and biomarker prevalence for papillary thyroid cancer in Japanese a-bomb survivors 1958 - 2005

Jan Christian Kaiser[a], Munechika Misumi[b] and Kyoji Furukawa[c]

[a]Helmholtz Zentrum München, Institute of Radiation Medicine,
85764 Oberschleißheim, Germany

[b]Department of Statistics, Radiation Effects Research Foundation,
732-0815 Hiroshima, Japan

[c]Biostatistics Center, Kurume University,
830-0011 Kurume, Japan

ARTICLE HISTORY

Compiled March 26, 2020

ABSTRACT

Purpose

Thyroid cancer of papillary histology (PTC) is the dominant type in radio-epidemiological cohorts established after nuclear accidents or warfare. Studies on post-Chernobyl PTC and on thyroid cancer in the life span study (LSS) of Japanese a-bomb survivors consistently revealed high radiation risk after exposure during childhood and adolescence. For post-Chernobyl risk assessment overexpression of the CLIP2 gene was proposed as molecular biomarker to separate radiogenic from sporadic PTC. Based on such binary marker a biologically-based risk model of PTC carcinogenesis has been developed for observational Chernobyl data. The model featured two independent molecular pathways of disease development, of which one was associated with radiation exposure. To gain credibility the concept for a mechanistic risk model must be based on general biological features which transcend findings in a single cohort. The purpose of the present study is therefore

CONTACT Jan Christian Kaiser. Email: christian.kaiser@helmholtz-muenchen.de

to demonstrate portability of the model concept by application to PTC incidence data in the LSS. By exploiting the molecular two-path concept we improve the determination of the probability of radiation causing cancer (POC).

Materials and methods

The current analysis uses thyroid cancer incidence data of the LSS with thyroid cancer diagnoses and papillary histology (n = 292) from the follow-up period between 1958 and 2005. Risk analysis was performed with both descriptive and biologically-based models.

Results

Judged by goodness-of-fit all applied models described the data almost equally well. They yielded similar risk estimates in cohorts post-Chernobyl and LSS. The preferred mechanistic model was selected by biological plausibility. It reflected important features of an imperfect radiation marker which are not easily addressed by descriptive models. Precise model predictions of marker prevalence in strata of epidemiological covariables can be tested by molecular measurements. Application of the radiation-related molecular pathway from our preferred model in retrospective risk assessment decreases the threshold dose for 50% POC from 0.33 (95% confidence interval (CI) 0.18; 0.64) Gy to 0.04 (95% CI 0.01; 0.19) Gy for females and from 0.43 (95% CI 0.17; 1.84) Gy to 0.19 (95% CI 0.05; 1.00) Gy for males. These improvements are still not sufficient to separate radiation-induced from sporadic PTC cases at very low doses < 0.015 Gy typical for the Fukushima accident.

Conclusions

Successful application of our preferred mechanistic model to LSS incidence data confirms and improves the biological two-path concept of radiation-induced PTC. Model predictions suggest further molecular validation studies to consolidate the basis of biologically-based risk estimation.

KEYWORDS

Papillary thyroid cancer; Radiation risk; Biomarker prevalence; Japanese a-bomb survivors; Mechanistic modeling of carcinogenesis

Introduction

Papillary thyroid cancer (PTC) is the most frequent histologic type in radioepidemiological cohorts of environmental exposure which have been established after nuclear accidents or warfare.

The Ukrainian-American (UkrAm) cohort and the Belorussian-American (BelAm) cohort were formed by subjects who were exposed as children or adolescents to ingested radio-iodine after the Chernobyl accident in 1986. Screening in both cohorts began in the late 1990s, absorbed thyroid doses were on average around 0.6 Gy, and a statistically significant dose response is well established (Brenner et al. 2011; Zablotska et al. 2011; Hatch and Cardis 2017). In the two post-Chernobyl cohorts more than 90% of thyroid cancers is of papillary histology (Bogdanova et al. 2015; Zablotska et al. 2015).

For the Life Span Study (LSS) of Japanese a-bomb survivors the radiation risk for papillary microcarcinoma of size < 1 cm has been found significantly enhanced in a subset of about 8,000 members with archived autopsy or surgical materials (Hayashi et al. 2010). Furukawa et al. (2013) performed their LSS analysis with incidence data 1958 - 2005 on all histologic types of thyroid cancer combined and reported an elevated radiation risk even 60 yr after exposure. Of their 371 thyroid cancer cases about 80 % had papillary histology. To avoid an influence of autopsy cases on risk estimates papillary microcarcinoma were excluded.

Radiation biomarkers have been sought for intensively in cancer tissue (Hall et al. 2017). The quest for radiation markers is arguably most advanced for PTC. Tissue samples have been prospectively collected in the Chernobyl Tissue Bank (CTB) from patients aged under 19 at the time of the accident and resident in highly contaminated areas of Ukraine and Russia. Molecular analysis of CTB samples suggested radiation-associated changes in genetic mutation profiles and transcriptomic data (Dom et al. 2012; Abend et al. 2013; Handkiewicz-Junak et al. 2016). Recently, Efanov et al. (2018) found driver gene mutations in almost all of 65 CTB patients which could be separated in two groups of typical genetic damage. Point mutations were associated with low thyroid doses of mean 0.2 Gy whereas gene fusions were found in highly exposed patients

with mean dose 1.4 Gy. Studies (Dom et al. 2012; Abend et al. 2013; Handkiewicz-Junak et al. 2016; Efanov et al. 2018) were mainly concerned with the molecular landscape of post-Chernobyl PTCs but did not connect with radioepidemiology.

A comprehensive analysis of molecular changes proposed overexpression of the CLIP2 gene as a radiation marker in post-Chernobyl PTC patients (Selmansberger et al. 2015a,b,c). A genomic network analysis revealed genes BAG2, CHST3, KIF3C, NEURL1, PPIL3 and RGS4 in the first neighborhood of CLIP2 suggesting the involvement of CLIP2 in the fundamental carcinogenic processes including apoptosis, mitogen-activated protein kinase signaling and genomic instability. PTC tissue originated partly from the CTB but also from members of the UkrAm cohort. Participation in a radioepidemiological cohort offered the unique opportunity to harness molecular patient data for radiation risk analysis. Kaiser et al. (2016) have developed a mechanistic risk model of PTC incidence in the UkrAm cohort using 115 PTC cases detected in four rounds of screening between 1999-2008. The model featured two independent pathways of CLIP2-associated carcinogenesis (C2C) and multi-stage carcinogenesis (MSC). Mechanistic modeling was used as a tool to characterize clinical and molecular properties associated with sporadic and radiation-induced PTC. Radiation risk in the UkrAm cohort was explained with a biologically-based dose response.

For a small number of LSS participants with PTC Hamatani et al. (2008) have linked RET/PTC rearrangements and BRAFV600E mutations to radiation exposure but comprehensive CLIP2 genotyping has not been performed in the LSS. Without sufficient molecular information it is still possible to transfer the biological concept of Kaiser et al. (2016) for a mechanistic risk model of radiation-induced PTC from the UkrAm cohort to the LSS. In this situation model results cannot be validated against molecular measurements but should be regarded as predictions for the outcome of such measurements. Therefore, the main purpose of the present study is to confirm and improve the biological model concept by application to LSS incidence data 1958 - 2005. Our study considers CLIP2 as a generic biomarker representing other radiation markers should they become available within epidemiological cohorts.

Recently, Preston (2015) identified adverse outcome pathways (AOPs) as a promising scientific framework to link basic radiobiological science with epidemiolog-

ical studies in radiation research. He advocated the application of biologically-based risk models which can provide the aspired methodological link to 'address uncertainty in low dose risk assessment' (Preston 2017; Rühm et al. 2017). The AOP concept originates from toxicology and describes disease development with a multi-scale approach (OECD 2013). Following up Preston's proposition we demonstrate possible improvements of accuracy in estimating the probability of radiation causing PTC in the Fukushima screening cohort conditioned on the availability of pertinent biomarkers (Fukushima Medical University 2017, 2018).

Materials and Methods

Life Span Study cohort

The Life Span Study (LSS) of Japanese atomic-bomb survivors has been one of the primary epidemiological sources for evaluating the long-term health effects of radiation exposure. The LSS cohort includes about 94,000 survivors who were in Hiroshima and Nagasaki at the time of bombing and about 27,000 people who were temporarily away from the cities at that time, and their mortality and cancer incidence have been followed up since 1950 and 1958, respectively (Ozasa et al. 2012; Grant et al. 2017). The current analysis used the thyroid cancer incidence data considered by Furukawa et al. (2013), for which thyroid cancer diagnoses and histologic types were identified by a panel of pathologists who examined records from the Hiroshima and Nagasaki tumor registries and histologic materials collected from area hospitals and pathology laboratories. During the follow-up period between 1958 and 2005, 371 first primary thyroid cancer cases were identified, of which 292 (79%) were papillary carcinomas. To avoid an influence of autopsy cases on risk estimates papillary microcarcinoma $<$ 1 cm were excluded Furukawa et al. (2013).

The data used in this analysis consisted of a table of case counts and person years finely cross-classified by city, gender, radiation dose, follow-up period, attained age, age at exposure, distance from the hypocenter, and the membership of the Adult Health Study (AHS) cohort (a clinical subset of the LSS cohort). Dose categories were defined in terms of weighted absorbed DS02 thyroid dose, which was calculated as the gamma-ray dose plus 10 times the neutron dose in Gy, with additional adjustment to reduce bias in risk estimates due to the uncertainty involved in individual dose estimation (Pierce et al. 1990; Cullings et al. 2006). Cohort details are summarized in Table S1 of the Supplementary Information (SI).

Descriptive models

State-of-the-art radioepidemiological (*descriptive*) risk models have been developed in the present study to assess risk estimates from mechanistic models. Model parameters have been deployed sparingly with the intention to capture only the important features

of age-risk patterns for PTC incidence. Models of excess relative risk (ERR) and of excess absolute rate (EAR) have been applied with functional forms given below.

The hazard function h_0 of sporadic PTC depends on sex s (subscript $_f$, $_m$ for females, males), birth year b, attained age a and AHS participation in the form

$$h_0(s, AHS, a, b) = \exp\left[b_s + b_{byr}\frac{(1935.6 - b)}{10} + b_a \ln(\frac{a}{60}) + b_{AHS}\right], \tag{1}$$

and expresses PTC incidence as cases in 10,000 persons per year (PY).

In the multiplicative model the total hazard $h_{ERR} = h_0 \cdot [1 + \text{ERR}]$ is determined by the Excess Relative Risk

$$\text{ERR}(D, s, e, a) = err\ D \cdot \exp\left[\pm p_s + p_e\frac{(e - 10)}{10} + p_a \ln(\frac{a}{60})\right] \tag{2}$$

for thyroid dose D with effect modifiers $+p_s$, $-p_s$ for females, males, age at exposure e and attained age a.

In the additive model with total hazard $h_{EAR} = h_0 + EAR$ the Excess Absolute Rate is given by

$$\text{EAR}(D, s, e, AHS) = ear\ D \cdot \exp\left[\pm p_s + p_e\frac{(e - 10)}{10} + b_{AHS}\right]. \tag{3}$$

The EAR quantifies the estimated radiation-induced excess cases per 10,000 PY. AHS participation is modeled with the same parameter b_{AHS} for h_0 and EAR.

Mechanistic models

Biological concept

Thyroid cancer is caused by a chain of processes which are not fully understood. They involve a large spatial scale from DNA level to the full organ and span a time period of decades. The mechanistic model only addresses a few main features of carcinogenesis which are rate-limiting for the incidence data. The biological basics for the mechanistic model have been laid out by Kaiser et al. (2016) and are summarized below.

The human thyroid contains about 10^{10} follicular cells (thyrocytes) but carcinogenesis would start from only about 0.1 % somatic stem cells with largely unknown molecular properties and functions (Bianconi et al. 2013; Dumont et al. 1992; Fierabracci 2012). The adult thyroid gland is a slowly proliferating organ with cells dividing once in 8.5–14.4 yr in order to maintain its size and function (Coclet et al. 1989). PTC is the most common histologic type which develops from unknown precursor cells.

According to the paradigm of multi-stage carcinogenesis (MSC) introduced by Takano (2017), these cells grow from N_c normal thyrocytes by acquiring genomic instability (Xing 2013). Typical oncogenic alterations related to MSC include point mutations in genes BRAF and RAS (Selmansberger et al. 2015a). Agrawal et al. (2014) provide a comprehensive genomic characterization of unexposed PTCs. Gradual expansion of initiated thyrocytes creates pre-neoplastic lesions which are transformed into PTC after acquiring a second oncogenic mutation [1].

To allow for radiation exposure, Takano (2017) proposed an independent model of PTC development starting with differentiated fetal thyroid cells (or thyroblasts), which disappear during adolescence. Kaiser et al. (2016) associated this model with CLIP2-related carcinogenesis (C2C) in a second pathway. They assumed that radiation initiates early genetic damage in thyroblasts which develop into PTC faster than in the MSC pathway. Radiation-induced clonal growth has not been included in C2C development of Kaiser et al. (2016). However, pre-neoplastic clones of initiated thyroblasts must be involved in carcinogenesis and are now modeled explicitly. Clones grow easily after radiation exposure, but in the absence of enhanced medical surveillance (screening) they do not become clinically relevant [2].

The model design with two independent molecular pathways of MSC and C2C is shown in Fig. 1. Both pathways are subject to genomic instability and deregulated intra-celluar MAPK signaling of intermediate cells. Sporadic PTCs can occur in both pathways but with different molecular signature. Radiation-induced PTCs are exclusively associated with the C2C pathway (Selmansberger et al. 2015a; Kaiser et al.

[1] Panels A, B of Fig. 1 in Takano (2017) represent PTC development along the MSC pathway.
[2] Panel C of Fig. 1 in Takano (2017) schematically depicts PTC development along the C2C pathway.

2016).

Model implementation

To date there is only sparse evidence for radiation markers of PTC from the LSS (Hamatani et al. 2008). Hence, mechanistic model development is mainly guided by goodness-of-fit and biological plausibility gained from previous UkrAm studies (Selmansberger et al. 2015c,a). The two-path model of Kaiser et al. (2016) is used as a starting point. Modifications and improvements in both legs of the two-path model were necessary and possible, since the LSS data contained more than twice the number of cases, which were recorded in a much longer follow-up period under a less rigorous regime of medical surveillance.

Without guidance from robust LSS biomarkers we did not develop a unique mechanistic model. We decided to present two viable mechanistic models M0 and M1 of PTC development with more emphasis on either improved goodness-of-fit (M0) or biological plausibility (M1). Both models apply the same hazard function in the sporadic MSC pathway given in Eq. (S1). For the second pathway the sparse model M0 applies a hazard of purely radiation-induced carcinogenesis (RIC). In *ideal* model M0 sporadic and radiation-induced PTC occur in mutually exclusive pathways MSC and RIC. Rich model M1 allows for both sporadic and radiation-induced PTC in the same C2C pathway as shown in Fig. 1. It complies with findings for the CLIP2 marker implemented in the full model of Kaiser et al. (2016). Model M1 uses three additional parameters compared to model M0 with 10 parameters. A condensed mathematical derivation for both models is given in the SI.

Probability of causation

The probability of causation $POC = h_r/h_{tot} = \mathrm{ERR}/(1+\mathrm{ERR})$ denotes the probability that a PTC is induced by radiation after clinical ascertainment. Radiation-induced hazard h_r and total hazard h_{tot} are estimated by radioepidemiological analysis. The probability of finding a molecular CLIP2 marker in PTC tissue P_{mol} of post-Chernobyl patients has a strong dose response (Selmansberger et al. 2015c). If binary CLIP2 sta-

tus were a perfect radiation marker it would separate sporadic PTC from radiation-induced PTC without any missclassification. For an ideal marker P_{mol} is equal to the probability of causation POC (Kaiser et al. 2016). This equivalence links molecular biology with radioepidemiology. We estimate POC in the present study because it can be directly compared with P_{mol} obtained in molecular studies by logistic regression on the biomarker status (Hamatani et al. 2008; Kaiser et al. 2016). Software packages such as ProZeS or IREP provide estimates of POC for retrospective risk assessment (Kocher et al. 2008; Ulanowski et al. 2016).

Statistical analysis

Statistical analysis was performed with the R software suite (R Core Team 2018). Model parameters were determined by Poisson regression based on the person year table of PTC incidence in the LSS. Maximum likelihood estimates for parameters of mechanistic models were calculated with R package `bbmle` (Bolker and Team 2017), for descriptive models R package `gnm` was applied (Turner and Firth 2015). Uncertainty ranges for risk estimates were determined by Monte-Carlo simulation based on the parameter correlation matrix, which is available if the Hessian matrix for the fit is positive definite. By matching the correlation matrix, multivariate normal parameter distributions of 10,000 realizations were simulated with function `mvrnorm` of R package `MASS` (Venables and Ripley 2002). Confidence intervals were picked as 2.5% and 97.5% percentiles from uncertainty distributions for risk estimates which were calculated from the simulated parameter realizations. Statistical significance for model parameters is stated based on likelihood ratio tests (LRTs) with a 95% confidence level. For single parameters p-values of 0.05 are applied correspondingly.

Results

Model selection

The preferred descriptive EAR and ERR models and the mechanistic two-path models M0 and M1 depend on the same covariables of sex, AHS participation, birth cohort, attained age, age at exposure and thyroid dose. Dependencies on city of residence Hiroshima or Nagasaki in the baseline of the descriptive models did not improve the fits based on LRTs and have not been considered further. Deviance and AIC (= deviance + 2 × no. of model parameters) for the preferred models are given in Table 1 . Maximum likelihood estimates (MLEs) for model parameters are given in Tables 2 to 5.

Exponential attenuation of the linear dose response in the higher dose range was not found significant for the ERR model (p-value 0.15). Attenuation was found significant in the EAR model (p-value 0.04) but has not been included since it disappeared (p-value 0.34) after removing just one case with thyroid dose > 3 Gy. Dose effect modifiers for sex (p-value 0.35) and attained age (p-value 0.38) in the ERR model have been kept to allow for comparison with other models. In the EAR model the dose effect modifier for attained age (p-value 0.08) has been dropped due to negligible influence. Differential increase by AHS participation of the baseline hazard (Eq. (1)) compared to the EAR (Eq. (3)) improved the deviance by less than a point and was not included in the EAR model.

Sex dependence in the sporadic MSC pathway of the mechanistic models M0 and M1 was significant for the clonal expansion rate γ_{MSC}, which is about twice as large for females compared to males. Age dependence (p-value 0.16) or exponential attenuation (p-value 0.07) of the dose response have not been included in the mechanistic model M0. As in the EAR model differential increase by AHS participation of the MSC hazard (Eq. (S4)) compared to the RIC hazard (Eq. (S10)) in model M0 slightly increased the AIC.

The baseline rate of clonal expansion γ_{C2C} in the C2C pathway for model M1 had to be fixed after minimization of the Poisson deviance to facilitate calculation of the parameter correlation matrix for confidence interval (CI) simulation. Based on goodness-of-fit permanent enhancement of clonal expansion after acute radiation

exposure as implemented in Eq. (S7) was identified as the preferred mechanism (Table 1).

Although model M1 was already slightly under-identified we allowed for the same radiation effect of Eq. (S7) in pathway MSC as in pathway C2C. With this extension the sensitivity of model M1 on the pathway-specific impact of radiation is tested. The radiation response parameter in the MSC pathway produces a small amount of 5 potentially radiation-induced cases in a total of 234 PTCs. With p-value 0.66 the extension of model M1 is not considered for the main analysis. In the C2C pathway of extended model M1 41 of 58 cases would have been induced by radiation. Compared to the *ideal* model M0 with sensitivity and specificity of the radiation biomarker equal to one, the corresponding values are 0.71, 1 (sensitivity, specificity) for model M1, and 0.71, 0.98 for model extended M1.

To confirm the two-path concept a mechanistic single path model has been tested by omitting the MSC leg of model M1 and replacing the step-wise dependence on age at exposure (Eq. (S6)) of the C2C leg by an exponential dependence on birth year as in Eq. (S4). Inferior goodness-of-fit excluded the single path model from further analysis (Table 1).

Mechanistic analysis is primarily performed with model M1 which we prefer based on biological plausibility. Supporting results from model M0 are cited from the SI.

Risk assessment

Fig. 2 shows estimates of ERR and EAR from mechanistic model M1 and from the descriptive models depending on age at exposure. In Fig. 3 the age dependence of the ERR averaged for both sexes is depicted for comparison with the UkrAm cohort. The left boundary for attained age is determined by the lowest person-year weighted mean age 18 yr for cases in the LSS, the right boundary includes the oldest PTC cases operated in the UkrAm cohort until 2015. Radiation risk estimates for mechanistic model M0 are very similar to those of model M1 albeit with slightly smaller CI. As an example, Fig. S2 shows the age dependence of the ERR for models M0, M1 and the ERR model. An overview of risk estimates for pertinent exposure scenarios is given in Table 6.

Estimates of sporadic PTC incidence from mechanistic models M0 and M1 are shown in Fig. S3. In view of pathway-specific analysis for biomarker prevalence it is important to note that baseline hazards of models M0 and M1 are almost identical for age > 20 yr.

Biomarker prevalence

Fig. 4 presents the number of PTC cases predicted by mechanistic model M1 in pathways MSC and C2C for categories of thyroid dose, attained age, age at exposure and time since exposure. The corresponding relative frequencies (Fig. S4) in each category provide complementary information on possible trends between categories which may not be visible for absolute case numbers. Figs. S5 and S6 show similar data for model M0 with pathways MSC and RIC. In Table S2 predictions by models M0 and M1 of case-related arithmetic means and standard deviations for the covariables are broken down by molecular pathways. Model predictions for pathways in total are compared with crude estimates from the LSS.

In Fig. 5 the probability of causation for the ERR model POC_{ERR} is plotted as a function of the thyroid dose. For model M1 the probability of causation can be expressed in two ways as a) $POC_{M1} = h_{rC2C}/h_{M1}$ with the total hazard h_{M1} of Eq. (S8) as denominator and b) $POC_{C2C} = h_{rC2C}/h_{C2C}$ just for the C2C pathway. Since $POC_{C2C} \geq POC_{M1}$ determination of the biomarker status for a PTC patient can increase the accuracy in separating radiation-induced cases from sporadic cases.

Discussion

Model M0 applies a simple radiation mechanism which generates a constant additive risk after acute exposure (Eq. (S10)). Model M1 relies on a more articulated mechanism of radiation-induced increase in clonal expansion (Eq. (S7)). The radiation mechanism of permanently increased proliferation in pre-neoplastic lesions was also found in LSS studies for breast cancer and lung adenocarcinoma (Kaiser et al. 2012; Castelletti et al. 2019). It may be related to radiation-induced protracted inflammation (Hayashi et al. 2012). A mechanistic explanation is based on radiation-induced cell inactivation. It assumes that cells initiated with genetic damage can replace inactivated cells in their immediate neighborhood faster than healthy cells (Heidenreich et al. 2001; Heidenreich and Paretzke 2008). Recently, such mechanism has been discovered in the esophagus of irradiated mice where TP53-initiated cells could clonally outgrow other epithelial cells while resisting radiation-induced oxidative stress (Fernandez-Antoran et al. 2019).

Model M1 produces a small number of 17 sporadic PTC in the C2C pathway which is, nevertheless, dominated by radiation action (Table S2). Sporadic PTCs with a positive CLIP2 marker have been observed in post-Chernobyl studies for patients operated at age > 20 yr (Selmansberger et al. 2015c).

Takano (2017) proposed fetal thyroid cells as targets of radiation-induced PTC development which disappear during adolescence. Implementing this assumption into the mechanistic model with a logistic step function yielded a vanishing radiation risk for exposure above age 30 yr. According to the mechanistic models 5-6 (about 1/8) of in total 44 radiation-induced PTC cases appeared in LSS members exposed between 18-29 yr (Figs. 4 and S5). The ERR model predicted in total 48 radiation-induced cases of which 8 (18%) were exposed between 18-29 yr and 2 (4%) above 30 yr. Radio-sensitivity decreased more rapidly with age at exposure according to the mechanistic models. Still, however, a non-negligible number of radiation-induced PTCs are generated for exposure after age 18 yr, which remain undetected in screening studies.

The biological two-path concept of Kaiser et al. (2016) has gained support from statistical association analysis in the LSS since the UkrAm model could be transferred to the LSS with adequate modification. However, based on goodness-of-fit we could

not decide if a potential biomarker is exclusively induced by radiation as in model M0 or if the markers occurs both sporadically *or* induced by radiation as in model M1. Occurrence of radiation-induced PTCs in the MSC pathway of model M1 lacks support by statistical significance but cannot be ruled out completely.

EAR estimates from mechanistic model M1 and the EAR model are in close agreement with EAR estimates for the UkrAm cohort (Table 6). Given the different intensity of screening regimes such behavior is surprising. Fig. 3 depicts sex-averaged ERR estimates from the LSS which are generally higher than UkrAm estimates. The discrepancy is caused by markedly lower baseline rates (Fig. S3) compared to the UkrAm cohort (Fig. S3 in Kaiser et al. (2016)).

Given the differences in screening regime, age structure and radiation exposure the characterization of PTC in the LSS for epidemiological covariables (Table S2) cannot be compared quantitatively with the UkrAm cohort (Table 3 of Kaiser et al. (2016)). However, Figs. 4 and S4 reveal trends consistent with those observed in the UkrAm cohort. Biomarker-positive PTCs are predicted not only for higher doses but also in unexposed subjects. Prevalence of positive status dominates for dose > 0.5 Gy and for attained age < 40 yr.

Hamatani et al. (2008) investigated RET/PTC rearrangements and BRAFV600E point mutations in PTC tissue of 71 a-bomb survivors of which 21 were not exposed to the bombings. PTC was diagnosed between 1956 - 1993. Both genetic alterations are mutually exclusive but are involved in deregulated MAPK signaling as oncogenic process in PTC precursor cells. Since BRAF mutations occur mainly sporadically they can be associated with the MSC pathway. The radiogenic origin of RET/PTC rearrangements is not fully clarified for post-Chernobyl PTC (Leeman-Neill et al. 2013; Selmansberger et al. 2015a; Kaiser et al. 2016), but seems to be supported in a-bomb survivors (Hamatani et al. 2008). To reconcile these ambiguous findings positive RET/PTC status could be assigned to the C2C pathway of model M1 which includes both sporadic and radiation-induced PTC.

For patients tested for RET/PTC status or BRAF status median values and ranges for covariables age at time of bombings, age at diagnosis, time since exposure and thyroid dose are given in Tables 2 and 3 of Hamatani et al. (2008). Comparison

with the corresponding covariables of Table S2 reveals agreement for positive status of RET/PTC and BRAF in covariables age at exposure and thyroid dose. For attained age and time since exposure quantitative agreement cannot be expected given the longer follow-up of the LSS in the present study. However, we can state that in the MSC pathway PTCs occur at older age at exposure and attained age and at markedly lower doses compared to PTC in the CSC pathway in line with the findings of Hamatani et al. (2008).

After the Fukushima accident about 300,000 residents aged < 19 yr in 2011 had ultrasound examinations of their thyroid gland. Full-scale thyroid screening started in April 2014, PTCs were detected almost exclusively in the first and second rounds of screening until 2017. Of 51 surgical cases only one case was classified with other histology (Fukushima Medical University 2017, 2018). External thyroid doses from the accident have been estimated below 15 mGy but dosimetry is incomplete (Fukushima Medical University 2016). The radiogenic origin of these cases is under debate (Tsuda et al. 2016; Yamashita et al. 2018). However, the matter should be clarified, since young PTC patients expect still a long life. In view of large uncertainties statistical association analysis at very low doses is pushed to its limits. But molecular biomarkers such as CLIP2 overexpression, gene rearrangements or indel/SNV ratios might potentially resolve the issue in retrospective risk assessment (Hamatani et al. 2008; Selmansberger et al. 2015b; Behjati et al. 2016; Efanov et al. 2018).

Perfect radiation markers have been assumed for model M0, but to date such biomarkers are not known. Slightly imprecise markers are more realistically involved in model M1. Therefore, positive marker status cannot guarantee absolute certainty for a radiogenic PTC, but still can be applied to obtain a more accurate probability of causation POC. For females POC_{M1} from total model M1 (and the ERR model) would exceed 50% chance of radiogenic PTC at about 0.33 Gy (Fig. 5). For a patient with a positive biomarker, we can discard all PTC with negative status for risk analysis, because they do not provide any radiation-related information.

As a consequence, POC_{C2C} just in the C2C pathway rises above POC_{M1} for the total model M1. Correspondingly, the threshold of 50% chance is markedly lowered from 0.33 (95% CI 0.18; 0.64) Gy to 0.04 (95% CI 0.01; 0.19) Gy for females and from

0.43 (95% CI 0.17; 1.84) Gy to 0.19 (95% CI 0.05; 1.00) Gy for males. At very low doses < 15 mGy MLEs for POC_{C2C} fall below 25% for females and below 6% for males. Such POC_{C2C} estimates do not support a robust association with radiation exposure. Missclassification errors from marker measurements are likely to further reduce POC_{C2C}. This example demonstrates the capability of radiation markers to improve retrospective risk assessment at low doses around 0.1 Gy. But at very low doses around 0.01 Gy improvements are still not sufficient to separate radiation-induced from sporadic cases.

Biologically-based modeling in relation to AOPs

Preston (2015) proposed to transfer of the AOP concept from toxicology to radiation research. For toxicologists Vinken et al. (2017) have given a brief summary. Their depiction of a generic AOP structure (their Figure 2) involves different levels of biological organization over many length scales. Disease development to an adverse outcome (AO) is understood as a linear chain of causes and effects which is triggered by a molecular initial event (MIE). A number of key events (KEs) are encountered along the path to an A0 which are in principle accessible to (radio-)biological or epidemiological investigation. Pathways MSC and C2C can be interpreted as AOPs with typical KEs of oncogenic mutations, clonal expansion or biomarker prevalence. Kaiser et al. (2016) have assessed molecular KEs such as copy number alterations, transcriptome expression, gene mutations and rearrangements in view of their association with pathways MSC and C2C. However, open questions remain since MIEs of PTC development in both pathways are not fully identified. But in the present study a comprehensive interpretation of the preferred mechanistic model in the AOP framework is beyond the scope.

Limitations and conclusions

In terms of goodness-of-fit both mechanistic and descriptive models explain PTC incidence in the LSS data almost equally well (Table 1). This fact complicates the selection of a preferred model for risk analysis because model selection cannot be based on statis-

tical association alone. Our choice of a preferred mechanistic model is therefore guided by biological plausibility even if model parameters are slightly under-identified. Based on evidence gained from the UkrAm cohort, our preferred model reflects realistic biological properties of an imperfect radiation marker such as CLIP2 overexpression which cannot be easily addressed by descriptive models. The lack of comprehensive information on molecular biomarkers for PTC in the LSS constitutes an obvious limitation of the present study because the preferred model cannot be immediately tested against measurements. However, our preferred model clearly predicts the prevalence of an imperfect radiation marker stratified by the classical epidemiological covariables of radiation dose, attained age, age at exposure and time since exposure. These model predictions, which descriptive models do not provide, are directly testable in future investigation.

As an important precondition the concept for a mechanistic risk model must be based on general biological features which are not exclusively related to a single cohort. By demonstrating the portability of the conceptual model between cohorts UkrAm and LSS, the resilience of biologically-based risk modeling has gained further credibility. With the Fukushima example we could show that informing biologically-based risk modeling with radiation markers can potential improve the accuracy of low dose risk assessment.

References

Abend M, Pfeiffer RM, Ruf C, Hatch M, Bogdanova TI, Tronko MD, Hartmann J, Meineke V, Mabuchi K, Brenner AV. 2013. Iodine-131 dose-dependent gene expression: alterations in both normal and tumour thyroid tissues of post-Chernobyl thyroid cancers. Br J Cancer. 109(8):2286–94.

Agrawal N, Akbani R, Aksoy BA, Ally A, Arachchi H, Asa SL, Auman JT, Balasundaram M, Balu S, Baylin SB, et al. 2014. Integrated Genomic Characterization of Papillary Thyroid Carcinoma. Cell. 159(3):676–690. Available from: http://www.sciencedirect.com/science/article/pii/S0092867414012380.

Behjati S, Gundem G, Wedge DC, Roberts ND, Tarpey PS, Cooke SL, Loo PV, Alexandrov LB, Ramakrishna M, Davies H, et al. 2016. Mutational signatures of ionizing radiation in second malignancies. Nat Commun. 7:12605.

Bianconi E, Piovesan A, Facchin F, Beraudi A, Casadei R, Frabetti F, Vitale L, Pelleri MC, Tassani S, Piva F, et al. 2013. An estimation of the number of cells in the human body. Ann Hum Biol. 40(6):463–71.

Bogdanova TI, Zurnadzhy LY, Nikiforov YE, Leeman-Neill RJ, Tronko MD, Chanock S, Mabuchi K, Likhtarov IA, Kovgan LM, Drozdovitch V, et al. 2015. Histopathological features of papillary thyroid carcinomas detected during four screening examinations of a Ukrainian-American cohort. Br J Cancer. 113(11):1556–64.

Bolker B, Team RDC. 2017. bbmle: Tools for General Maximum Likelihood Estimation. R package version 1.0.20; Available from: https://CRAN.R-project.org/package=bbmle.

Brenner AV, Tronko MD, Hatch M, Bogdanova TI, Oliynik VA, Lubin JH, Zablotska LB, Tereschenko VP, McConnell RJ, Zamotaeva GA, et al. 2011. I-131 dose response for incident thyroid cancers in Ukraine related to the Chornobyl accident. Environ Health Perspect. 119(7):933–9.

Castelletti N, Kaiser JC, Simonetto C, Furukawa K, Kuechenhoff H, Stathopoulos G. 2019. Risk of lung adenocarcinoma from smoking and radiation arises in distinct molecular pathways. Carcinogenesis.

Coclet J, Foureau F, Ketelbant P, Galand P, Dumont JE. 1989. Cell population kinetics in dog and human adult thyroid. Clin Endocrinol (Oxf). 31(6):655–65.

Cullings HM, Fujita S, Funamoto S, Grant EJ, Kerr GD, Preston DL. 2006. Dose estimation for atomic bomb survivor studies: its evolution and present status. Radiat Res. 166(1 Pt 2):219–54. Available from: http://www.ncbi.nlm.nih.gov/pubmed/16808610.

Dom G, Tarabichi M, Unger K, Thomas G, Oczko-Wojciechowska M, Bogdanova T, Jarzab B, Dumont JE, Detours V, Maenhaut C. 2012. A gene expression signature distinguishes normal tissues of sporadic and radiation-induced papillary thyroid carcinomas. Br J Cancer. 107(6):994–1000.

Dumont JE, Lamy F, Roger P, Maenhaut C. 1992. Physiological and pathological regulation of thyroid cell proliferation and differentiation by thyrotropin and other factors. Physiol Rev. 72(3):667–97.

Efanov AA, Brenner AV, Bogdanova TI, Kelly LM, Liu P, Little MP, Wald AI, Hatch M, Zurnadzy LY, Nikiforova MN, et al. 2018. Investigation of the Relationship Between Radiation Dose and Gene Mutations and Fusions in Post-Chernobyl Thyroid Cancer. J Natl Cancer Inst. 110(4):371–378.

Fernandez-Antoran D, Piedrafita G, Murai K, Ong SH, Herms A, Frezza C, Jones PH. 2019. Outcompeting p53-Mutant Cells in the Normal Esophagus by Redox Manipulation. Cell Stem Cell. 25(3):329–341.e6.

Fierabracci A. 2012. Identifying thyroid stem/progenitor cells: advances and limitations. J Endocrinol. 213(1):1–13.

Fukushima Medical University. 2016. Basic Survey, Appendix (Estimated external radiation dose. Fukushima city 960-1295, Japan: Office of International Cooperation, Radiation Medical Science Center. Available from: http://fmu-global.jp/download/appendix-estimated-external-radiation-dose-16/.

Fukushima Medical University. 2017. Thyroid Ultrasound Examination (First Full-Scale Thyroid Screening Program). Fukushima city 960-1295, Japan: Office of International Cooperation, Radiation Medical Science Center. Available from: http://fmu-global.jp/download/thyroid-ultrasound-examination-first-full-scale-thyroid-screening-program-3/.

Fukushima Medical University. 2018. Thyroid Ultrasound Examinations (Second Full-Scale Thyroid Screening Program). Fukushima city 960-1295, Japan: Office of International Cooperation, Radiation Medical Science Center. Available from: http://fmu-global.jp/download/thyroid-ultrasound-examinations-second-full-scale-thyroid-screening-program/.

Furukawa K, Preston D, Funamoto S, Yonehara S, Ito M, Tokuoka S, Sugiyama H, Soda M, Ozasa K, Mabuchi K. 2013. Long-term trend of thyroid cancer risk among Japanese atomic-bomb survivors: 60 years after exposure. International Journal of Cancer. 132(5):1222–6.

Grant EJ, Brenner A, Sugiyama H, Sakata R, Sadakane A, Utada M, Cahoon EK, Milder CM, Soda M, Cullings HM, et al. 2017. Solid Cancer Incidence among the Life Span Study of Atomic Bomb Survivors: 1958-2009. Radiat Res. 187(5):513–537.

Hall J, Jeggo PA, West C, Gomolka M, Quintens R, Badie C, Laurent O, Aerts A, Anastasov N, Azimzadeh O, et al. 2017. Ionizing radiation biomarkers in epidemiological studies - An update. Mutat Res. 771:59–84.

Hamatani K, Eguchi H, Ito R, Mukai M, Takahashi K, Taga M, Imai K, Cologne J, Soda M, Arihiro K, et al. 2008. RET/PTC rearrangements preferentially occurred in papillary thyroid cancer among atomic bomb survivors exposed to high radiation dose. Cancer Research. 68(17):7176–82.

Handkiewicz-Junak D, Swierniak M, Rusinek D, Oczko-Wojciechowska M, Dom G, Maenhaut C, Unger K, Detours V, Bogdanova T, Thomas G, et al. 2016. Gene signature of the post-Chernobyl papillary thyroid cancer. Eur J Nucl Med Mol Imaging. 43(7):1267–77.

Hatch M, Cardis E. 2017. Somatic health effects of Chernobyl: 30 years on. Eur J Epidemiol. 32(12):1047–1054.

Hayashi T, Morishita Y, Khattree R, Misumi M, Sasaki K, Hayashi I, Yoshida K, Kajimura J, Kyoizumi S, Imai K, et al. 2012. Evaluation of systemic markers of inflammation in atomic-bomb survivors with special reference to radiation and age effects. FASEB J. 26(11):4765–73.

Hayashi Y, Lagarde F, Tsuda N, Funamoto S, Preston DL, Koyama K, Mabuchi K, Ron E, Kodama K, Tokuoka S. 2010. Papillary microcarcinoma of the thyroid among atomic bomb survivors: tumor characteristics and radiation risk. Cancer. 116(7):1646–55.

Heidenreich WF, Atkinson M, Paretzke HG. 2001. Radiation-induced cell inactivation can increase the cancer risk. Radiat Res. 155(6):870–2.

Heidenreich WF, Paretzke HG. 2008. Promotion of initiated cells by radiation-induced cell inactivation. Radiation Research. 170(5):613–7. Available from: http://www.ncbi.nlm.nih.gov/pubmed/18959457.

Kaiser JC, Jacob P, Meckbach R, Cullings HM. 2012. Breast cancer risk in atomic bomb survivors from multi-model inference with incidence data 1958-1998. Radiation and Environmental Biophysics. 51(1):1–14. Available from: http://www.ncbi.nlm.nih.gov/pubmed/21947564.

Kaiser JC, Meckbach R, Eidemüller M, Selmansberger M, Unger K, Shpak V, Blettner M, Zitzelsberger H, Jacob P. 2016. Integration of a radiation biomarker into modeling of thyroid carcinogenesis and post-Chernobyl risk assessment. Carcinogenesis. 37(12):1152–1160.

Kocher DC, Apostoaei AI, Henshaw RW, Hoffman FO, Schubauer-Berigan MK, Stancescu DO, Thomas BA, Trabalka JR, Gilbert ES, Land CE. 2008. Interactive RadioEpidemiological Program (IREP): a web-based tool for estimating probability of causation/assigned share of radiogenic cancers. Health Phys. 95(1):119–47. Available from: http://www.ncbi.nlm.nih.gov/pubmed/18545036.

Leeman-Neill RJ, Brenner AV, Little MP, Bogdanova TI, Hatch M, Zurnadzy LY, Mabuchi K, Tronko MD, Nikiforov YE. 2013. RET/PTC and PAX8/PPARγ chromosomal rearrangements in post-Chernobyl thyroid cancer and their association with iodine-131 radiation dose and other characteristics. Cancer. 119(10):1792–9.

OECD. 2013. Guidance document on developing and assessing adverse outcome pathways, in Environment Directorate Joint Meeting of the Chemicals Committee and the Working Party on Chemicals; Organization for Economic Co-operation and Development (OECD); Paris.

Ozasa K, Shimizu Y, Suyama A, Kasagi F, Soda M, Grant EJ, Sakata R, Sugiyamaa H, Kodama K. 2012. Studies of the Mortality of Atomic Bomb Survivors, Report 14, 1950-2003: An Overview of Cancer and Noncancer Diseases. Radiation Research. 177:229–243.

Pierce DL, Væth M, Stram DO. 1990. Allowing for random errors in radiation dose estimates for the atomic bomb survivor data. Radiation Research. 170:118–126.

Preston RJ. 2015. Integrating basic radiobiological science and epidemiological studies: why and how. Health Physics. 108(2):125–30.

Preston RJ. 2017. Can radiation research impact the estimation of risk? Int J Radiat Biol. 93(10):1009–1014.

R Core Team. 2018. R: A Language and Environment for Statistical Computing. Vienna, Austria: R Foundation for Statistical Computing. Available from: https://www.R-project.org/.

Rühm W, Eidemüller M, Kaiser JC. 2017. Biologically-based mechanistic models of radiation-related carcinogenesis applied to epidemiological data. Int J Radiat Biol. 93(10):1093–1117.

Selmansberger M, Braselmann H, Hess J, Bogdanova T, Abend M, Tronko M, Brenner A, Zitzelsberger H, Unger K. 2015a. Genomic copy number analysis of Chernobyl papillary thyroid carcinoma in the Ukrainian-American Cohort. Carcinogenesis. 36(11):1381–7.

Selmansberger M, Feuchtinger A, Zurnadzhy L, Michna A, Kaiser JC, Abend M, Brenner A, Bogdanova T, Walch A, Unger K, et al. 2015b. CLIP2 as radiation biomarker in papillary thyroid carcinoma. Oncogene. 34(30):3917–25.

Selmansberger M, Kaiser JC, Hess J, Güthlin D, Likhtarev I, Shpak V, Tronko M, Brenner A,

Abend M, Blettner M, et al. 2015c. Dose-dependent expression of CLIP2 in post-Chernobyl papillary thyroid carcinomas. Carcinogenesis. 36(7):748–56.

Takano T. 2017. Natural history of thyroid cancer [Review]. Endocr J. 64(3):237–244.

Tronko M, Brenner AV, Bogdanova T, Shpak V, Oliynyk V, Cahoon EK, Drozdovitch V, Little MP, Tereshchenko V, Zamotayeva G, et al. 2017. Thyroid neoplasia risk is increased nearly 30 years after the Chernobyl accident. Int J Cancer. 141(8):1585–1588.

Tsuda T, Tokinobu A, Yamamoto E, Suzuki E. 2016. Thyroid Cancer Detection by Ultrasound Among Residents Ages 18 Years and Younger in Fukushima, Japan: 2011 to 2014. Epidemiology. 27(3):316–22.

Turner H, Firth D. 2015. Generalized nonlinear models in R: An overview of the gnm package. R package version 1.0-8; Available from: http://CRAN.R-project.org/package=gnm.

Ulanowski A, Eidemüller M, Güthlin D, Kaiser JC, Shemiakina E, Jacob P. 2016. Quantitative Abschätzung des Strahlenrisikos unter Beachtung individueller Expositionsszenarien, Teil 2 - ProZES: a tool for assessment of assigned share of radiation in probability of cancer development (Part II). Bundesamt für Strahlenschutz (BfS). Report No:. Http://nbn-resolving.de/urn:nbn:de:0221-2016112214169.

Venables WN, Ripley BD. 2002. Modern Applied Statistics with S. 4th ed. New York: Springer. ISBN 0-387-95457-0; Available from: http://www.stats.ox.ac.uk/pub/MASS4.

Vinken M, Knapen D, Vergauwen L, Hengstler JG, Angrish M, Whelan M. 2017. Adverse outcome pathways: a concise introduction for toxicologists. Arch Toxicol. 91(11):3697–3707.

Xing M. 2013. Molecular pathogenesis and mechanisms of thyroid cancer. Nat Rev Cancer. 13(3):184–99.

Yamashita S, Suzuki S, Suzuki S, Shimura H, Saenko V. 2018. Lessons from Fukushima: Latest Findings of Thyroid Cancer After the Fukushima Nuclear Power Plant Accident. Thyroid. 28(1):11–22.

Zablotska LB, Nadyrov EA, Rozhko AV, Gong Z, Polyanskaya ON, McConnell RJ, O'Kane P, Brenner AV, Little MP, Ostroumova E, et al. 2015. Analysis of thyroid malignant pathologic findings identified during 3 rounds of screening (1997-2008) of a cohort of children and adolescents from Belarus exposed to radioiodines after the Chernobyl accident. Cancer. 121(3):457–66.

Zablotska LB, Ron E, Rozhko AV, Hatch M, Polyanskaya ON, Brenner AV, Lubin J, Romanov GN, McConnell RJ, O'Kane P, et al. 2011. Thyroid cancer risk in Belarus among children and adolescents exposed to radioiodine after the Chornobyl accident. Br J Cancer.

104(1):181–7.

Figures

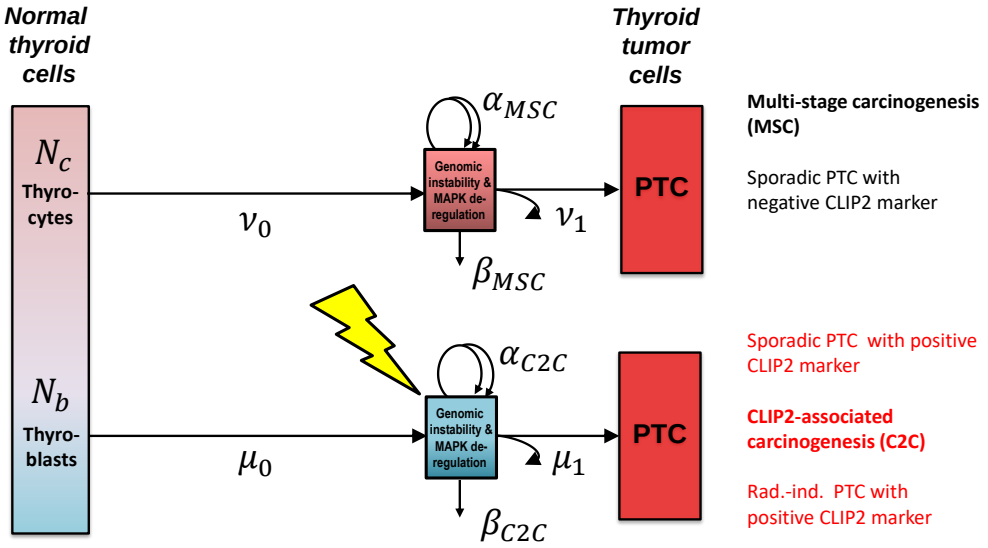

Figure 1. Conceptual model M1 for the development of sporadic PTC from multi-stage carcinogenesis (MSC) (upper path) and sporadic *or* radiation-induced PTC from CLIP2-associated carcinogenesis (C2C) (lower path), a mathematical formulation of the model is given in the SI, PTC development starts from either N_c thyrocytes in the MSC pathway or N_b thyroblasts in the C2C pathway (left box), small central boxes in MSC and C2C pathways represent clones of intermediate cells with genomic instability and deregulated MAPK signaling; arrows between boxes indicate Poisson point processes for asymmetrically dividing cells using Greek letters ν, μ as transition rates; α, β denote rates of symmetric cell division and inactivation in pre-neoplastic clones, radiation exposure (jagged yellow arrow) targets intermediate cells in the C2C pathway and permanently enhances their growth rate $\gamma_{C2C} \approx \alpha_{C2C} - \beta_{C2C}$ (Eqns. (S5) and (S7)), molecular changes in PTC tissue (right boxes) are discussed in Selmansberger et al. Selmansberger et al. (2015a).

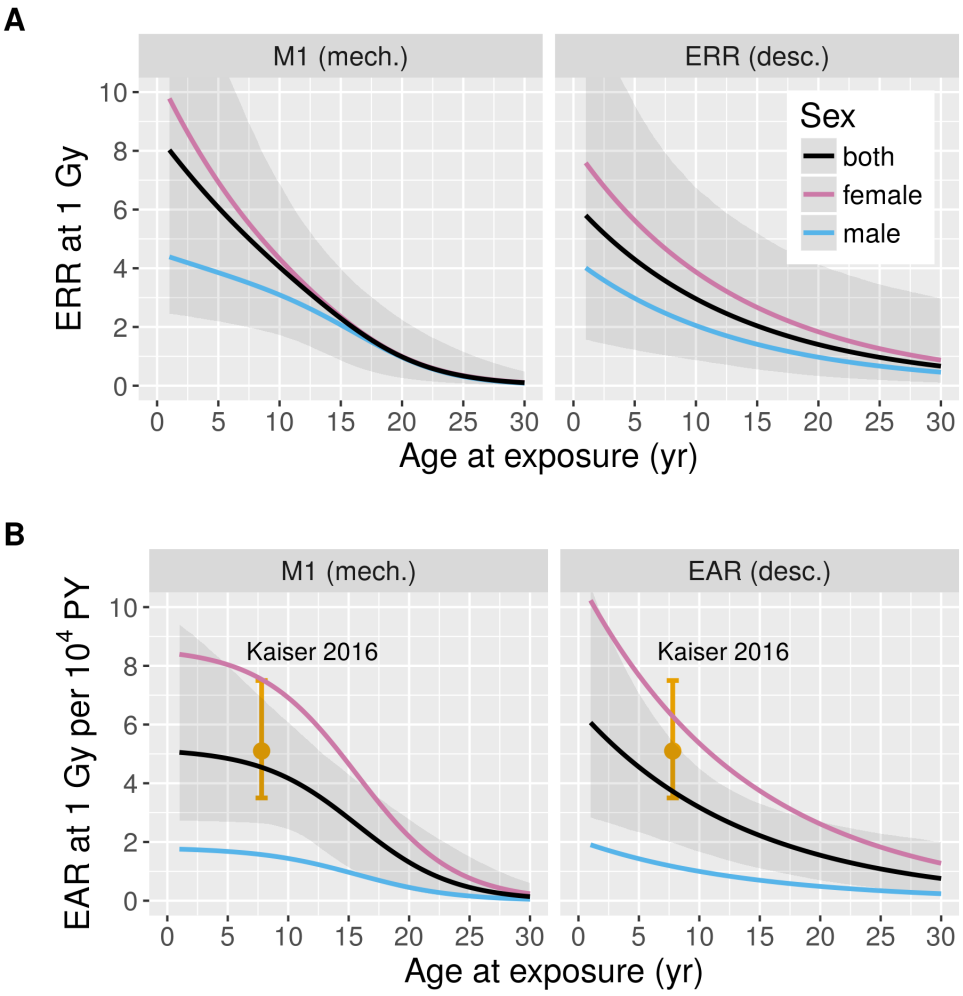

Figure 2. **A** ERR at 1 Gy and **B** EAR at 1 Gy per 10,000 PY for females, males and averaged for both sexes 30 yr after exposure from the mechanistic model M1 (left panels), and from the descriptive models ERR (right upper panel) and EAR (right lower panel), 95% CI are shaded for sex averages, point estimate and 95 %CI of the EAR averaged for both sexes from the mechanistic model of Kaiser et al. (2016) for the UkrAm cohort at mean age at exposure 8 yr.

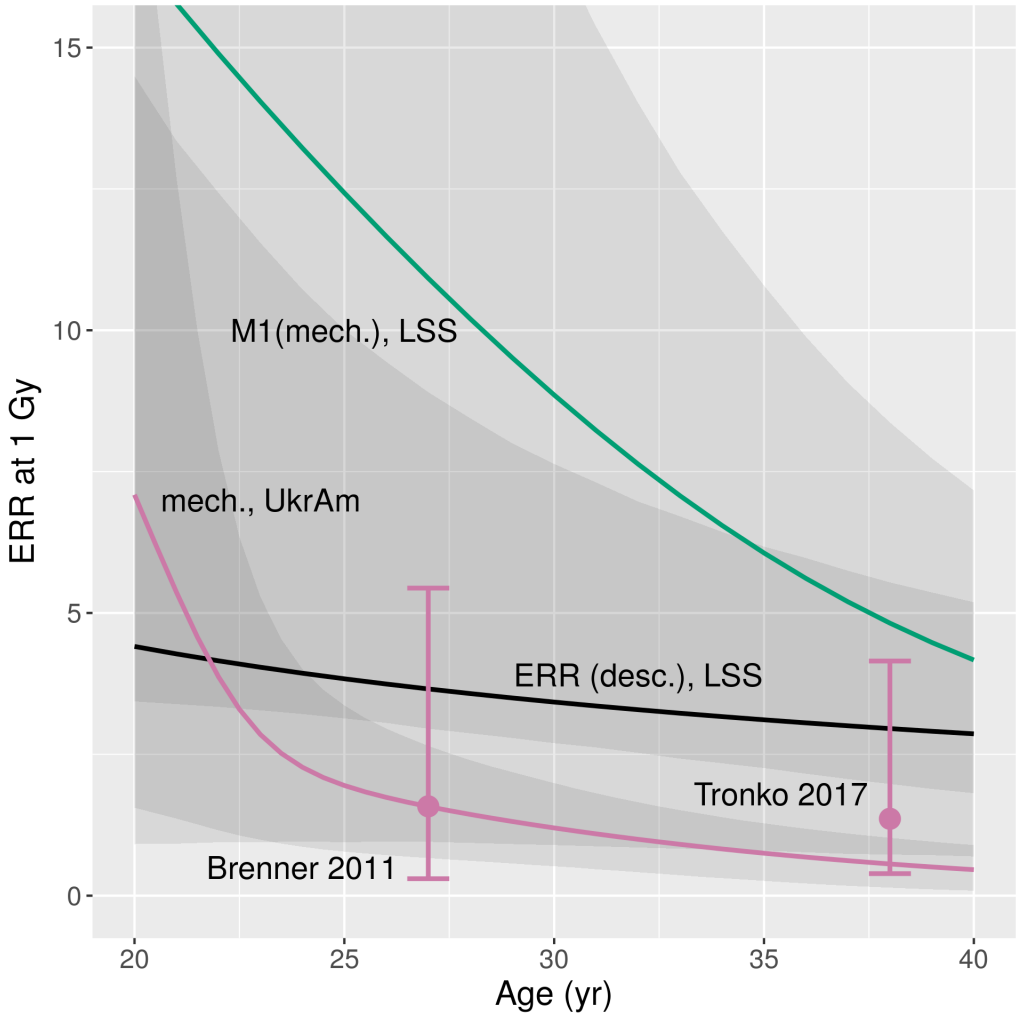

Figure 3. Sex-averaged ERR at 1 Gy with shaded 95% CI from the mechanistic model M1 and the descriptive ERR model for the LSS at age at exposure 8 yr, and from the mechanistic model for the UkrAm cohort (mean age at exposure 8 yr) of Kaiser et al. (2016); for comparison ERR estimates from the UkrAm studies of Brenner et al. (2011) for mean age at operation 27 yr and of Tronko et al. (2017) (all histologic types) for mean age at operation 38 yr are shown.

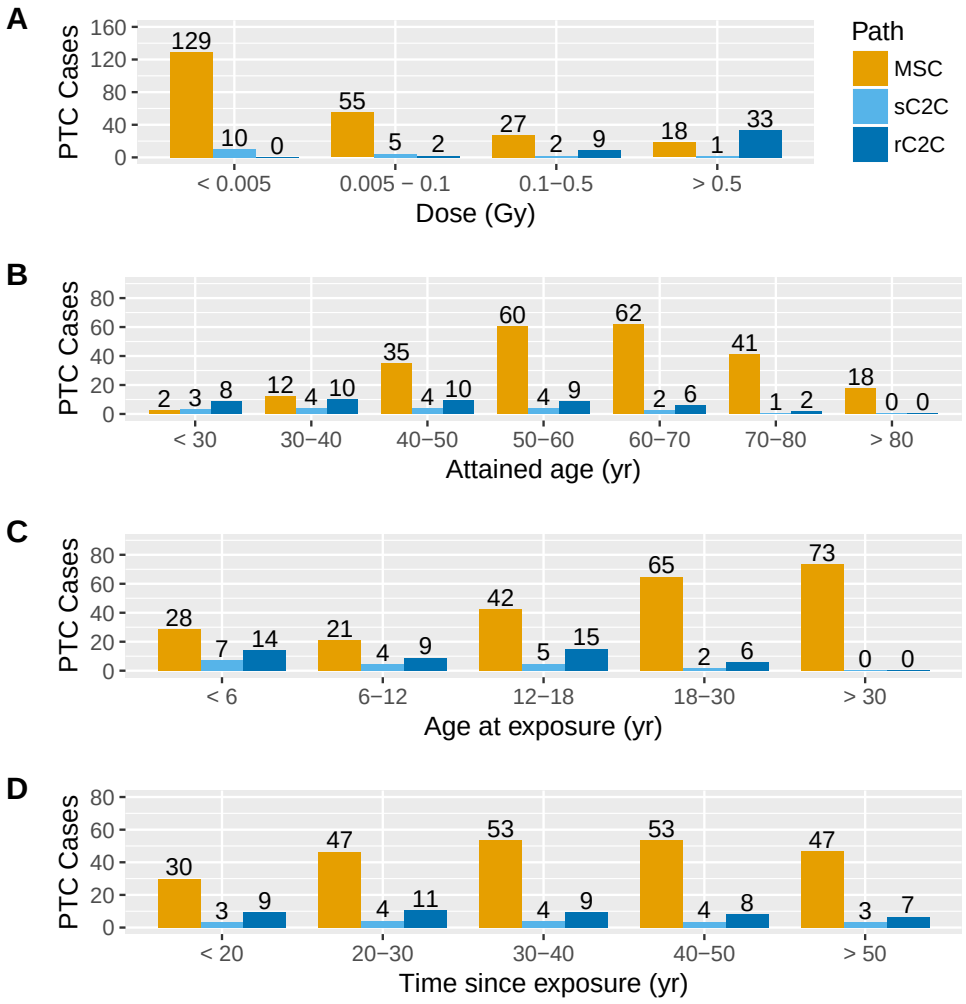

Figure 4. Number of PTC cases predicted by mechanistic model M1 in pathways MSC and C2C for categories of **A** thyroid dose, **B** attained age, **C** age at exposure and **D** time since exposure, in the MSC pathway PTC cases develop only sporadically, in the C2C pathway PTC cases develop either sporadically (sC2C) or induced by radiation (rC2C).

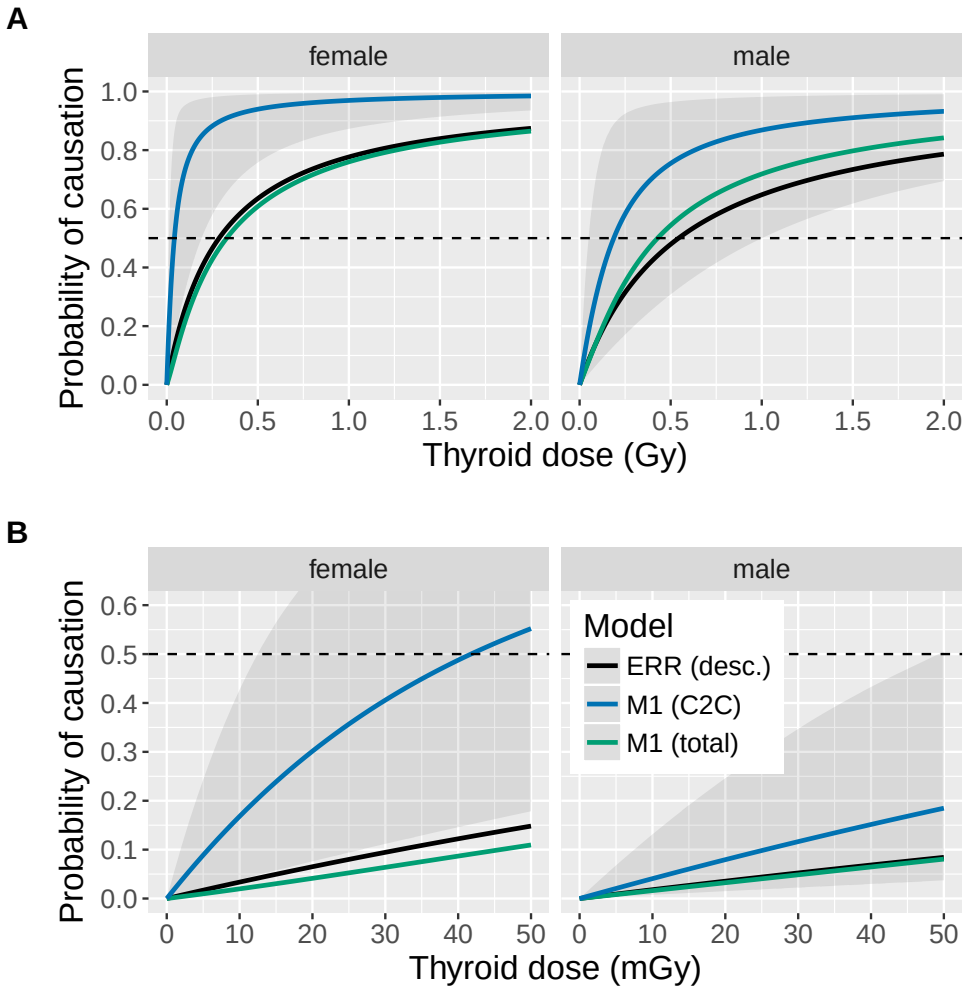

Figure 5. Probability of causation *POC* for females and males at attained age 45 yr after exposure at 8 yr from the descriptive ERR model, from the total mechanistic model M1 and from the mechanistic model M1 within the CSC pathway only (shaded 95% CI) in dose ranges **A** 0 - 2 Gy, **B** 0 - 50 mGy, for males the total M1 model and the ERR model yield the same result in the low dose range.

Tables

Table 1. Deviance, number of adjustable parameters N_{par} and AIC = deviance $+2N_{par}$ for the preferred descriptive ERR and EAR models, the mechanistic two-path models M0 and M1, and the mechanistic single path model SP, for model M1 different radiation targets have been tested, lowest values of deviance and AIC are marked in bold, preferred model M1 with radiation-induced promotion permanently enhanced in the C2C pathway is applied for the main analysis based on biological plausibility.

Model	deviance	N_{par}	AIC	
descriptive				dose effect modifiers
ERR	3006.8	9	3024.8	attained age, age at exposure, sex
EAR	3009.1	8	3025.1	age at exposure, sex
mechanistic				radiation action
M0	3003.4	10	**3023.4**	initiation rate μ_0, acute (1 week)
[a]M1	**3002.5**	13	3028.5	promotion rate γ_{C2C}, permanent, Eq. (S7)
M1	3002.2	14	3030.2	promo. rate γ_{C2C}, γ_{MSC}, permanent, Eq. (S7)
M1	3007.4	13	3033.4	promotion rate γ_{C2C}, acute (1 week)
M1	no convergence			initiation rate μ_0, permanent
M1	3006.1	13	3032.1	initiation rate μ_0, acute (1 week)
SP	3018.6	7	3032.6	promotion rate γ, permanent, Eq. (S7)

[a] preferred model M1

Table 2. Maximum likelihood estimates (MLEs), standard errors, p-values and significance codes for parameters of the descriptive ERR model from Eqns. (1), (2).

Name	MLE	std. err.	p-value	sign. code
b_f	0.410	0.113	0.00029	**
b_m	-0.701	0.189	0.00021	**
b_a	1.54	0.29	$< 10^{-4}$	***
b_{byr}	-0.254	0.059	$< 10^{-4}$	***
b_{AHS}	0.700	0.147	$< 10^{-4}$	***
err	2.06	0.79	0.0090	**
[a]p_s	0.318	0.343	0.35	-
p_e	-0.727	0.278	0.0089	**
p_a	-0.623	0.705	0.38	-

[a] $+p_s$ for females, $-p_s$ for males
significance codes for p-values
$< 10^{-4}$: ***, $\geq 10^{-4} - < 0.01$: **,
$\geq 0.01 - < 0.05$: *, $\geq 0.05 - < 0.1$: ., > 0.1: -

Table 3. Maximum likelihood estimates (MLEs), standard errors, p-values and significance codes for parameters of the descriptive EAR model from Eqns. (1), (3), AHS participation is modeled with the same parameter b_{AHS} for baseline and EAR.

Name	MLE	std. err.	p-value	sign. code
b_f	0.447	0.111	$< 10^{-4}$	$***$
b_m	-0.674	0.186	$< 10^{-4}$	$***$
b_a	1.64	0.28	$< 10^{-4}$	$***$
b_{byr}	-0.276	0.060	$< 10^{-4}$	$***$
ear	1.16	0.37	0.0018	$**$
[a]p_s	0.841	0.290	0.0041	$**$
p_e	-0.718	0.240	0.0028	$**$
b_{AHS}	0.690	0.150	$< 10^{-4}$	$***$

[a] $+p_s$ for females, $-p_s$ for males
significance codes for p-values
$< 10^{-4}$: $***$, $\geq 10^{-4} - < 0.01$: $**$,
$\geq 0.01 - < 0.05$: $*$, $\geq 0.05 - < 0.1$: ., > 0.1: -

Table 4. Maximum likelihood estimates (MLEs), standard errors, p-values and significance codes for parameters of the mechanistic model M0, pertaining to pathways of either multi-stage carcinogenesis (MSC) or radiation-induced carcinogenesis (RIC), AHS adjustment is applied to both pathways combined.

pathway	name	unit	MLE	std. err.	p-value	sign. code
MSC	[a]X_{MSC}	yr^{-2}	-15.55	0.70	$< 10^{-4}$	$***$
	γ_{MSC}	yr^{-1}	0.0777	0.0226	0.00059	$**$
	[b]p_{MSC}	-	0.336	0.084	$< 10^{-4}$	$***$
	[a]δ_{MSC}	yr^{-2}	-9.25	0.48	$< 10^{-4}$	$***$
	b_{byr}	-	-0.240	0.056	$< 10^{-4}$	$***$
RIC	x_d	$10^{-4}(\mathrm{Gy\ PY})^{-1}$	1.92	0.72	0.0075	$**$
	[b]p_{C2C}	-	0.762	0.271	0.0050	$**$
	b_{slp}	yr	7.37	5.76	0.20	-
	e_{cen}	yr	15.6	4.5	0.00048	$**$
both	b_{AHS}	-	0.703	0.145	$< 10^{-4}$	$***$

[a] log-transformed

[b] $+p$ for females, $-p$ for males

significance codes for p-values

$< 10^{-4}$: $***$, $\geq 10^{-4} - < 0.01$: $**$,

$\geq 0.01 - < 0.05$: $*$, $\geq 0.05 - < 0.1$: ., > 0.1: -

Table 5. Maximum likelihood estimates (MLEs), standard errors, p-values and significance codes for parameters of the preferred mechanistic model M1 pertaining to pathways of either multi-stage carcinogenesis (MSC) or CLIP2-associated carcinogenesis (C2C), radiation permanently enhances clonal expansion in the C2C pathway after exposure according to Eq. (S7), AHS adjustment is applied to both pathways combined.

pathway	name	unit	MLE	std. err.	p-value	sign. code
MSC	[a]X_{MSC}	yr^{-2}	-17.0	1.9	$< 10^{-4}$	$***$
	γ_{MSC}	yr^{-1}	0.112	0.046	0.015	$*$
	[b]p_{MSC}	-	0.292	0.069	$< 10^{-4}$	$***$
	[a]δ_{MSC}	yr^{-2}	-10.2	1.4	$< 10^{-4}$	$***$
	b_{byr}	-	-0.210	0.061	0.00055	$**$
C2C	[a]X_{C2C}	yr^{-2}	-14.2	1.5	$< 10^{-4}$	$***$
	γ_{C2C}	yr^{-1}	0.0217	fixed		N/A
	g_d	Gy^{-1}	50.902	0.035	$< 10^{-4}$	$***$
	[b]p_{C2C}	-	0.751	0.256	0.0034	$**$
	[a]δ_{C2C}	yr^{-2}	-5.59	1.58	0.00041	$**$
	b_{slp}	yr	7.97	5.25	0.13	-
	e_{cen}	yr	15.7	4.3	0.00025	$**$
both	b_{AHS}	-	0.693	0.146	$< 10^{-4}$	$***$

[a] log-transformed
[b] $+p$ for females, $-p$ for males
significance codes for p-values
$< 10^{-4}$: $***$, $\geq 10^{-4} - < 0.01$: $**$,
$\geq 0.01 - < 0.05$: $*$, $\geq 0.05 - < 0.1$: ., > 0.1: -

Table 6. MLE estimates of the EAR and ERR (95% CI) for age at exposure 8 yr from mechanistic model M1 in the LSS, descriptive models EAR and ERR in the LSS, and for mean age at exposure 8 yr from the mechanistic model in the UkrAm cohort (Kaiser et al. 2016).

	EAR (PTC cases per 10,000 PY at 1 Gy)				
	model M1			EAR model	mech., UkrAm
	male	female	sex average	sex average	sex average
	1.6 (0.49; 3.9)	7.5 (3.9; 11)	4.5 (2.4, 6.8)	3.7 (2.0; 5.8)	5.1 (3.5; 7.5)
	ERR at 1 Gy				
age	model M1			ERR model	mech., UkrAm
(yr)	male	female	sex average	sex average	sex average
35	3.9 (0.63; 11)	6.9 (2.8; 13)	6.1 (2.3; 11)	2.6 (0.80; 4.5)	0.75 (0.26; 1.3)
60	1.4 (0.32; 3.5)	2.1 (1.1; 4.0)	1.9 (1.0; 3.3)	2.6 (0.80; 4.5)	-

Declaration of interest

The author declares no conflict of interest.

Biographical note

Dr Jan Christian Kaiser leads the working group "Integrative Modeling" in the Institute of Radiation Medicine at the Helmholtz Zentrum München, German Research Center for Environmental Health, in Munich, Germany. He holds a doctoral and masters' degree in statistical physics. His research involves integration of molecular biology and radiation epidemiology in biologically-based risk models.

Dr Munechika Misumi is the Associate Senior Scientist in the Department of Statistics, Radiation Effects Research Foundation in Hiroshima, Japan. He has a Ph.D. and a Master of Statistics with biomedical concentration. He has been involved in a variety of epidemiological and biological studies based on the cohort of atomic bomb survivors. His research interests include statistical methodologies for radiation epidemiology, measurement errors in the regression analysis, and biological modeling.

Dr. Kyoji Furukawa is a professor at Biostatistics Center, Kurume University, Japan. He has been a researcher in biostatistics and radiation research, and his recent interests include methodological development for radiation risk assessment.